

# Unpaired and spin-singlet paired states of a two-dimensional electron gas in a perpendicular magnetic field

M. Polini<sup>1</sup>, K. Mouloupoulos<sup>2</sup>, B. Davoudi<sup>1,3</sup> and M. P. Tosi<sup>1</sup>

<sup>1</sup>*NEST-INFM and Classe di Scienze, Scuola Normale Superiore, I-56126 Pisa, Italy*

<sup>2</sup>*Department of Physics, University of Cyprus, P.O. Box 20537, 1678 Nicosia, Cyprus*

<sup>3</sup>*Institute for Studies in Theoretical Physics and Mathematics, Tehran 19395-5531, Iran*

We present a variational study of both unpaired and spin-singlet paired states induced in a two-dimensional electron gas at low density by a perpendicular magnetic field. It is based on an improved circular-cell approximation which leads to a number of closed analytical results. The ground-state energy of the Wigner crystal containing a single electron per cell in the lowest Landau level is obtained as a function of the filling factor  $\nu$ : the results are in good agreement with those of earlier approaches and predict  $\nu_c \approx 0.25$  for the upper filling factor at which the solid-liquid transition occurs. A novel localized state of spin-singlet electron pairs is examined and found to be a competitor of the unpaired state for filling factor  $\nu > 1$ . The corresponding phase boundary is quantitatively displayed in the magnetic field-electron density plane.

PACS number: 73.20.Dx, 73.40.Hm

## I. INTRODUCTION

The nature of the ground-state of a two-dimensional (2D) many-electron system in a perpendicular magnetic field has been for a number of years a subject of intense experimental and theoretical investigation. Since the discovery of the Integer and Fractional Quantum Hall Effects<sup>1</sup>, this has been one of the richest sources of fundamental new physics in Condensed Matter. The transition from a liquid to a Wigner crystal (WC) state, originating from strong electron-electron correlations at low density in strong magnetic fields, has received considerable attention (see *e.g.* Ref. 2 and references given therein). More recently, novel and intriguing behaviors of 2D electron transport in high Landau levels have been reported<sup>3</sup>. In such regime of weak magnetic fields Koulakov *et al.*<sup>4</sup> predicted that charge density waves (CDW) would break the translational symmetry in one direction and form stripes. They also predicted stabilization of a novel 2D-CDW state with more than one electron per unit cell. Such a “bubble” phase arising from spin-triplet electron pair formation and 2D lattice ordering has been confirmed in systematical numerical studies of Haldane *et al.*<sup>5</sup> and of Shibata and Yoshioka<sup>6</sup>.

In the present work we introduce a new possible low-temperature phase for a 2D electron system in a perpendicular magnetic field, namely a localized paired-electron state consisting of a spin-singlet electron pair in each cell, and investigate its stability at low densities against the more conventional WC state containing a single electron per cell. We have in mind situations where the Zeeman splitting can be neglected<sup>7</sup>. In free space, where the Landé  $g$ -factor of an electron is  $g = 2$ , the Zeeman splitting is exactly equal to the cyclotron splitting. It turns out, however, that this is incorrect, for example, in a GaAs heterostructure for the following reasons: (i) the small effective mass in the conduction band increases the cyclotron energy by a factor of  $m/m^* \sim 14$ ; (ii) the effective coupling of the electron spin to the external magnetic field is reduced by spin-orbit scattering by a factor of  $-5$ , making the effective Landé factor  $g \sim -0.4$ . Thus the Zeeman energy is about 70 times smaller than the cyclotron energy<sup>7</sup>.

This study has two main motivations. Firstly, from the solution of the simple problem of two-electrons moving on a plane under parabolic confinement<sup>8</sup> it emerges that the effective radial potential for the relative motion develops a pronounced minimum at sufficiently weak field. The minimum occurs even in the case of vanishing angular momentum ( $m = 0$ ) and is the result of the competition between the Coulomb repulsion and the localizing effects of the magnetic field and of the confinement. This feature may hide, in the many-body context and at sufficiently low electron densities, some new phase transition to a spin-singlet (for  $m = 0$ ) paired electron state in weak magnetic fields. Secondly, and following early work on a  $m = 0$  paired state in the 3D electron gas<sup>9</sup>, such a state was found in a variational calculation<sup>10</sup> to be a possible competitor to the conventional 3D-WC in zero field. A mixed spin state with a preference for spin pairing has been proposed to occur in some regions of the liquid phase from experiments on 2D electron systems in the ultra-quantum limit<sup>11</sup>.

In our evaluation of the energetics of the paired state we introduce an improved circular-cell approximation for an interacting 2D electron gas on a uniform positive background. We first study by this approach the conventional unpaired-electron WC state in a magnetic field<sup>12</sup>. Each electron is treated as a distributed charge cloud, which can

be taken to a good approximation to be localized within a cell if the density is not too high and the field is not too small – the radius of the circular cell being available as an additional variational parameter<sup>13</sup>. Our results are in close agreement with those obtained in earlier approaches. We then adopt a similar method to deal with two interacting electrons within each circular cell. This yields new and more complex expressions leading to a window of thermodynamic stability for the paired-electron state at higher values of the electron density.

The layout of the paper is briefly as follows. In Section II we present our treatment of the energy of the unpaired-electron 2D-WC in a magnetic field and compare our results with earlier ones and with the energy of the Laughlin liquid state. Section III summarizes the main results for the problem of two electrons moving in a plane under an applied magnetic field. Section IV reports our treatment of the singlet-paired state and Section V gives a variational calculation of the energy of this state and a determination of the phase boundary between the unpaired and the singlet-paired states. Finally, Section VI summarizes our main conclusions. Some technical points of detail are worked out in an Appendix.

## II. DISTRIBUTED-CHARGE APPROACH TO THE WIGNER CRYSTAL IN A MAGNETIC FIELD

A 2D system of carriers in a pure semiconductor sample subject to a magnetic field  $B$  is expected to undergo a transition to an ordered triangular lattice structure at sufficiently low temperature  $T$  and filling factor  $\nu$ <sup>14</sup>. Here,  $\nu = 2\pi n_s \ell^2$  where  $n_s$  is the areal carrier density and  $\ell = (\hbar c/eB)^{1/2}$  is the magnetic length. The ground-state energy of such a 2D-WC has been evaluated by a number of authors with various methods. In the following we shall indicate by  $\delta\epsilon$  the values of the ground-state energy after subtraction of the energy of the lowest Landau Level (LL).

The leading term of a low-density expansion is given by a classical Madelung-potential calculation<sup>15</sup>, leading to  $\delta\epsilon_{\text{class}} = -2.212206 r_s^{-1} \text{Ryd}^* = -0.782133 \nu^{1/2} (e^2/\epsilon \ell)$  where  $\epsilon$  is the dielectric constant of the host medium and  $r_s a_B^* = (\pi n_s)^{-1/2}$  with  $\text{Ryd}^*$  and  $a_B^*$  the effective Rydberg and Bohr radius. Following early Hartree-Fock calculations<sup>16</sup> and a classical-plasma simulation for the determination of the energy of the Laughlin liquid<sup>17</sup>, a variational calculation based on a correlated magnetophonon wave-function for the WC<sup>18</sup> gave the result

$$\delta\epsilon_{\text{CWC}} = -0.782133 \nu^{1/2} + 0.2410 \nu^{3/2} + 0.16 \nu^{5/2} (e^2/\epsilon \ell) \quad (1)$$

and predicted that the crystal energy would be lower than that of the liquid only at values of  $\nu$  lower than  $\nu_c \approx 0.14$ . Subsequent work by Vignale<sup>19</sup> used Current-Density Functional Theory in the projected local-density approximation and located the upper filling factor for the liquid-solid transition at  $\nu_c \approx 0.25$ , in fairly good agreement with the experimental evidence.

In our approach we model the 2D interacting electron system on a uniform positive background as a collection of non-interacting disks, each having a Wigner-Seitz radius  $r_{\text{ws}}$  to be eventually treated as a variational parameter and containing a single electron in a trial wave function with a variational width parameter  $\sigma$ . Specifically, we adopt a Gaussian trial wave function normalized to unity,

$$\phi_{\text{SP}}(r) = (\pi\sigma^2)^{-1/2} \exp(-r^2/2\sigma^2) \quad (2)$$

The single-particle density thus is  $\rho(r) = \phi_{\text{SP}}^2(r)$ . Taking the areal density of the background as  $\rho_b(r) = n_s \theta(r_{\text{ws}} - r)$ , the total electronic charge inside the disk radius is determined by

$$\int d^2r \phi_{\text{SP}}^2(r) \theta(r_{\text{ws}} - r) = 1 - \exp(-r_{\text{ws}}^2/\sigma^2) \quad (3)$$

and we must require  $\sigma \ll r_{\text{ws}}$  in order to avoid charge leakage errors. As noted by Nagy<sup>13</sup>, the handling of  $r_{\text{ws}}$  as a variational parameter ensures that the error involved in setting the electrical potential outside the disk to zero is minimized.

### A. Electron-background and background-background interaction energy

The potential energy  $V_{\text{in}}(r)$  created by the positive background inside the circular cell is given in terms of the Gauss hypergeometric function  $F(a, b; c; d)$  by<sup>13</sup>

$$V_{\text{in}}(r) = \frac{4}{r_s} F\left(\frac{1}{2}, -\frac{1}{2}; 1; r^2/r_{\text{ws}}^2\right) \frac{r_{\text{ws}}}{r_s a_B^*} \text{Ryd}^*. \quad (4)$$

This result is equivalent to the more familiar expression

$$V_{\text{in}}(r) = \frac{8}{\pi r_s} E(r^2/r_{\text{ws}}^2) \frac{r_{\text{ws}}}{r_s a_B^*} Ryd^* \quad (5)$$

where  $E(x)$  is the complete elliptic integral of the first kind (see Ref. 20, p. 591).

The self-interaction energy of the background is thus given by

$$\epsilon_{bb}(r_s, r_{\text{ws}}) = \frac{1}{2} \int d^2r \rho_b(r) V_{\text{in}}(r) = \frac{16}{3\pi r_s} \left( \frac{r_{\text{ws}}}{r_s a_B^*} \right)^3 Ryd^*, \quad (6)$$

having used the result  $\int_0^1 E(x^2) x dx = 2/3$ . Similarly, the interaction energy of the electron with the background is

$$\begin{aligned} \epsilon_{eb}(r_s, r_{\text{ws}}, \sigma) &= 2\pi \int_0^{r_{\text{ws}}} r dr \phi_{\text{SP}}^2(r) V_{\text{in}}(r) \\ &= -\frac{16 r_{\text{ws}}}{\pi r_s^2 a_B^*} \int_0^{r_{\text{ws}}/\sigma} x E(\sigma^2 x^2/r_{\text{ws}}^2) e^{-x^2} dx Ryd^*. \end{aligned} \quad (7)$$

For  $\sigma \ll r_{\text{ws}}$  Eq. (7) can be replaced by the approximate analytic expression

$$\epsilon_{eb}(r_s, r_{\text{ws}}, \sigma) = \left[ -\frac{4}{r_s} \frac{r_{\text{ws}}}{r_s a_B^*} + \frac{1}{r_s^3} \frac{(\sigma/a_B^*)^2}{(r_{\text{ws}}/r_s a_B^*)} \right] Ryd^*. \quad (8)$$

This so-called harmonic approximation (HA) for the electron-background energy is obtained from Eq. (7) by extending the range of integration up to  $\infty$  and by using the expansion of the elliptic integral  $E(x) = (\pi/2)(1 - x/4) + o(x^2)$  (see 20, p. 591).

An alternative way to calculate the electron-background energy is by using the expression

$$\epsilon_{eb}(r_s, r_{\text{ws}}, \sigma) = 2\pi \int_0^{r_{\text{ws}}} \rho_b(r) V_{\text{SP}}(r) r dr, \quad (9)$$

where  $V_{\text{SP}}(r)$  is the electrical potential created by a single electron in the state (2). This can be obtained in closed form,

$$V_{\text{SP}}(r) = -\frac{2\sqrt{\pi}}{(\sigma/a_B^*)} \exp(-r^2/2\sigma^2) I_0(r^2/2\sigma^2) Ryd^* \quad (10)$$

where  $I_n(x)$  is the modified Bessel function of the  $n$ -th order (see Appendix). The evaluation of Eq. (9) can then be carried out in closed form, with the result

$$\epsilon_{eb}(r_s, r_{\text{ws}}, \sigma) = -\frac{2\sqrt{\pi}}{(\sigma/a_B^*)} \left( \frac{r_{\text{ws}}}{r_s a_B^*} \right)^2 \exp(-r_{\text{ws}}^2/2\sigma^2) [I_0(r_{\text{ws}}^2/2\sigma^2) + I_1(r_{\text{ws}}^2/2\sigma^2)] Ryd^* \quad (11)$$

(see Appendix). The expression (8) is recovered from Eq. (11) for  $r_{\text{ws}} \gg \sigma$  by using the asymptotic expansion of the Bessel functions (see 20, p. 377). We shall see below that the ‘‘anharmonic corrections’’ implied by Eq. (11) are crucial in a comparison with earlier calculations.

## B. Total energy and variational procedure

The total energy per electron in a perpendicular magnetic field  $\mathbf{B}$  is

$$\epsilon_t = \epsilon_k(\sigma, B) + \epsilon_{eb}(r_s, r_{\text{ws}}, \sigma) + \epsilon_{bb}(r_s, r_{\text{ws}}) \quad (12)$$

where  $\epsilon_k(\sigma, B)$  is the kinetic energy,

$$\begin{aligned} \epsilon_k(\sigma, B) &= \int d^2r \phi_{\text{SP}}(r) \frac{1}{2m^*} \left( \mathbf{p} + \frac{e}{c} \mathbf{A} \right)^2 \phi_{\text{SP}}(r) \\ &= 2\pi \int_0^{+\infty} r \phi_{\text{SP}}(r) \left[ -\frac{\hbar^2}{2m^* r} \partial_r(r \partial_r) + \frac{1}{2} m^* \omega_0^2 r^2 \right] \phi_{\text{SP}}(r) dr \end{aligned} \quad (13)$$

with  $\omega_0 = eB/2m^*c$ . We have taken the vector potential in the symmetric gauge,  $\mathbf{A} = \mathbf{B} \times \mathbf{r}/2$ , and used the fact that the wave function (2) is an isotropic state of zero angular momentum. Eq. (13) yields

$$\epsilon_k(\sigma, B) = \left[ \frac{1}{(\sigma/a_B^*)^2} + \lambda_B \left( \frac{\sigma}{a_B^*} \right)^2 \right] Ryd^* \quad (14)$$

where  $\lambda_B \equiv m^* \omega_0^2 a_B^{*2} / (2 Ryd^*) \simeq 3.6 \cdot 10^{-12} (\epsilon m/m^*)^4 (B/\text{Tesla})^2$ . For a GaAs heterostructure we have  $\lambda_B \simeq 0.4$  if  $B = 10$  Tesla.

Equation (12), after insertion of Eqs. (6), (11) and (14) is minimized numerically with respect to the variational parameters  $\Sigma = \sigma/a_B^*$  and  $\alpha = r_{ws}/r_s a_B^*$ . The equilibrium values of these parameters are shown in Figure 1 as functions of  $r_s$  for two values of the magnetic field. The ratio  $\bar{\Sigma}/r_s \bar{\alpha} = (\sigma/r_{ws})_{eq}$  should be appreciably smaller than unity for internal self-consistency and the extent to which this consistency criterion is satisfied is shown in Figure 2. It is evident from Figures 1 and 2 that for these values of the field the harmonic approximation is applicable for the estimation of the variational parameters whenever the consistency criterion  $\bar{\Sigma}/r_s \bar{\alpha} \ll 1$  is satisfied.

Figure 3 reports our results for the ground-state energy  $\delta\epsilon_t$  as a function of the filling factor in the lowest LL, after subtraction of the kinetic energy  $2\lambda_B^{1/2} Ryd^*$  from the total energy  $\epsilon_t$  and rescaling to  $e^2/\epsilon\ell$  energy units. The left panel in Figure 3 shows that  $\delta\epsilon_t$  in these units is still weakly dependent on the field intensity at values of  $\nu$  larger than about 0.4. The right panel in Figure 3 compares our results for  $\delta\epsilon_t$  in the range  $0 < \nu \leq 0.5$  with those obtained in the correlated Wigner crystal approach of Lam and Girvin<sup>18</sup> (see Eq. (1)). It is also seen that the classical limit of Bonsall and Maradudin<sup>15</sup> is approximately recovered for  $\nu \rightarrow 0$ .

It is also seen from Figure 3 (left panel) that the ground-state energy of the unpaired WC as obtained in the present approach crosses the energy of the Laughlin liquid as reported by Levesque *et al.*<sup>17</sup> at  $\nu \approx 0.25$ . This value for the upper critical filling factor of the liquid-solid transition agrees with that reported by Vignale<sup>19</sup> and, as discussed by this author, there is strong experimental evidence supporting the fact that the crystal exists even at filling factors as large as 0.22-0.23<sup>2,21</sup>. However, again as discussed by Vignale, it appears that the liquid-solid transition is not a simple crossing of two phases occurring at a single value of  $\nu$ . Rather, it shows a complex reentrant behavior, with the liquid phase being stable at or near the Fractional Quantum Hall Effect fractions and the solid phase being stable in between.

We would also like to remark that the simple choice  $\alpha = 1$ , which ensures that the Wigner-Seitz cell is electrically neutral, implies only small changes relative to the prescription proposed by Nagy<sup>13</sup>. We in fact find that when we take  $\alpha = 1$  the critical filling factor at which the liquid-solid transition occurs shifts from  $\nu \approx 0.25$  to  $\nu \approx 0.23$ .

Finally, we briefly comment on the issue of Landau Level Mixing (LLM), as studied in detail by Zhu and Louie<sup>22</sup> and by Price *et al.*<sup>23</sup>. LLM is important when the ratio between the magnetic energy (of order  $\hbar\omega_0$ ) and the Coulomb energy (of order  $e^2/(\epsilon r_s a_B^*)$ ) becomes smaller than unity, *i.e.* for  $r_s < \lambda_B^{-1}$ . This effect is included in our approach through the use of a trial wave function having a variational width<sup>23</sup> and becomes unimportant as  $r_s$  increases and  $\sigma_{eq}$  approaches the value  $\sqrt{2}\ell$  for which Eq. (2) becomes the exact lowest-energy eigenfunction of the single-particle Hamiltonian. This asymptotic behavior is clearly seen from Figure 1 (left panel).

### C. Analytic results in the harmonic approximation

Having assessed numerically the range of validity of the harmonic approximation (HA) for the estimation of the model variational parameters, we proceed to report a number of analytic results which follow from it. The ground-state energy is given by

$$\epsilon_t^{\text{HA}} = \left( \Sigma^{-2} + \lambda_B \Sigma^2 - \frac{4\alpha}{r_s} + \frac{\Sigma^2}{\alpha r_s^3} + \frac{16\alpha^3}{3\pi r_s} \right) Ryd^*. \quad (15)$$

Minimization of Eq. (15) with respect to  $\Sigma$  and  $\alpha$  yields the results shown in Figure 1.

Let us consider first the choice  $\alpha = 1$  (*i.e.*  $r_{ws} = r_s a_B^*$ ), where the equilibrium value of  $\Sigma$  is

$$\bar{\Sigma}_{\alpha=1}(r_s, B) = \frac{r_s^{3/4}}{(1 + \lambda_B r_s^3)^{1/4}}. \quad (16)$$

Thus,  $\bar{\Sigma}_{\alpha=1}(r_s, B)$  decreases with increasing field, due to increased localization of the electron inside the circular cell, and saturates to the value  $\lambda_B^{-1/4}$  corresponding to  $\sigma_{eq} = (\hbar/m^* \omega_0)^{1/2}$ . The total energy per electron becomes

$$\epsilon_t^{\text{HA}}(r_s, B) = \left[ 2 \frac{(1 + \lambda_B r_s^3)^{1/2}}{r_s^{3/2}} + \left( \frac{16}{3\pi} - 4 \right) \frac{1}{r_s} \right] Ryd^* \quad (17)$$

and increases with the magnetic field, saturating to the value

$$\epsilon_t^{\text{HA}}(r_s, B \rightarrow \infty) = \left[ 2\lambda_B^{1/2} + \left( \frac{16}{3\pi} - 4 \right) \frac{1}{r_s} \right] Ryd^*. \quad (18)$$

The first term in the brackets in Eq. (18) is the cyclotron zero-point energy  $\hbar\omega_0$ . On the other hand, in the limit of vanishing field Eq. (17) yields

$$\begin{aligned} \epsilon_t^{\text{HA}}(r_s, B = 0) &= \left[ \left( \frac{16}{3\pi} - 4 \right) \frac{1}{r_s} + \frac{2}{r_s^{3/2}} \right] Ryd^* \\ &\simeq \left( -\frac{2.30}{r_s} + \frac{2}{r_s^{3/2}} \right) Ryd^*, \end{aligned} \quad (19)$$

which is the result obtained by Seidl *et al.*<sup>24</sup> in their ‘‘PC model’’ (the correlation energy is obtained from Eq. (19) by subtracting from it the exchange energy term given by  $-8\sqrt{2}/(3\pi r_s)$ ). The dependence of  $\epsilon_t^{\text{HA}}(r_s, B = 0)$  in Eq. (19) on the density parameter  $r_s$  is correct, but the numerical coefficients are somewhat different from those which are precisely known for the WC in zero field<sup>15</sup>. It may be remarked that the expression for  $\epsilon_t^{\text{HA}}(r_s, B = 0)$  in 3D provides a lower bound to the energy of the WC<sup>25</sup>.

Minimization of the energy in Eq. (15) with respect to  $\alpha$  is intended to approximately correct for the fact that the electrical potential in 2D does not vanish outside the circular cell and is expected to yield a variational lower bound for the ground-state energy<sup>13</sup>. The equilibrium value of the reduced Gaussian width is given by an expression similar to Eq. (16),

$$\bar{\Sigma}_{\bar{\alpha}}(r_s, B) = \left( \frac{\bar{\alpha} r_s^3}{1 + \bar{\alpha} \lambda_B r_s^3} \right)^{1/4} \quad (20)$$

while  $\bar{\alpha}$  converges with increasing  $r_s$  to the value  $\sqrt{\pi}/2$  (see Figure 1). That is, Nagy’s result<sup>13</sup>  $r_{\text{ws}} = (\sqrt{\pi}/2)r_s a_B^*$  remains valid in the presence of a magnetic field at low electron density. The expression for the ground-state energy becomes

$$\epsilon_t^{\text{HA}}(r_s, B) = \left[ 2\sqrt{2} \frac{(1 + \lambda_B \sqrt{\pi} r_s^3/2)^{1/2}}{\pi^{1/4} r_s^{3/2}} - \frac{4\sqrt{\pi}}{3} \frac{1}{r_s} \right] Ryd^*. \quad (21)$$

However, this simple analytic expression for the energy of the unpaired WC in a magnetic field is not sufficiently accurate on the energy scale needed for the comparisons made in Figure 3.

### III. MOTION OF AN ELECTRON PAIR IN A MAGNETIC FIELD

In this section we motivate the introduction of a paired state for the WC by discussing the spin-singlet ground-state and effective interaction potential for two electrons moving in a plane under a perpendicular magnetic field. As is known from the work of Taut<sup>8</sup>, this is an example of a quasi-exactly soluble problem with a hidden  $sl_2$ -algebraic structure<sup>26</sup>: an exact solution exists for special values of the field. Our aim will be to use the analytic form of the wave function determined in such a case in order to make a reasonable *Ansatz* for the variational treatment which will be developed for the paired phase in the next Section.

The Hamiltonian describing the two electrons is written in terms of the relative coordinate  $\mathbf{r} = \mathbf{r}_2 - \mathbf{r}_1$ , of the center-of-mass coordinate  $\mathbf{R} = (\mathbf{r}_1 + \mathbf{r}_2)/2$  and of the corresponding momenta  $\mathbf{p}$  and  $\mathbf{P}$  as

$$\mathcal{H} = \frac{1}{4m} \left[ \mathbf{P} + \frac{e}{c} \mathbf{A}_{\text{CM}}(\mathbf{R}) \right]^2 + \frac{1}{m} \left[ \mathbf{p} + \frac{e}{c} \mathbf{A}_{\text{rel}}(\mathbf{r}) \right]^2 + \frac{e^2}{r} + \mathcal{H}_{\text{spin}} \quad (22)$$

where  $\mathbf{A}_{\text{CM}}(\mathbf{R}) = \mathbf{B} \times \mathbf{R}$ ,  $\mathbf{A}_{\text{rel}}(\mathbf{r}) = \mathbf{B} \times \mathbf{r}/4$  and  $\mathcal{H}_{\text{spin}} = -(ge\hbar/mc)(\mathbf{s}_1 + \mathbf{s}_2)$  with  $\mathbf{s}_i$  being the spins. The addition of a harmonic confining potential merely shifts the value of the cyclotron frequency<sup>8</sup>. The center-of-mass motion in the ground-state is described by a Gaussian wave function having width given by the magnetic length  $\ell = (\hbar c/eB)^{1/2}$ . The wave function  $\phi_{\text{rel}}(\mathbf{r})$  for the relative motion in the spin-singlet ground-state is even under space inversion. Following the treatment developed by Taut<sup>8</sup>, an analytic expression is obtained for the state of zero relative angular momentum ( $M_{\text{rel}} = 0$ ) if the magnetic field satisfies the condition  $\gamma = 1$ , where  $\gamma \equiv \ell_{\text{rel}}/a_B$  with  $\ell_{\text{rel}} = \sqrt{2}\ell$  and  $a_B = \hbar^2/me^2$ . This state lies at relative energy  $2\hbar\omega_0$  and apart from a normalization factor is

$$\phi_{\text{rel}}(\mathbf{r}) \propto (1 + x) e^{-x^2/4} \quad (23)$$

with  $x = r/\ell_{\text{rel}}$ . This is, in fact, the solution which corresponds to the lowest value of  $\gamma$  and to the lowest energy.

Two main points of this two-electron problem need emphasizing. Firstly, the effective potential  $V_{\text{eff}}(r)$  entering the Schrödinger equation for the reduced wave function  $f_{\text{eff}}(\mathbf{r}) = \phi_{\text{rel}}(\mathbf{r}) \sqrt{r}$  at  $M_{\text{rel}} = 0$  is

$$V_{\text{eff}}(r) = \frac{1}{4}x^2 + \frac{\gamma}{x} - \frac{1}{4x^2} \quad (24)$$

and develops a minimum for  $\gamma > (16/27)^{1/4}$  (see Figure 4). This fact will motivate the introduction of the paired phase in the next Section. Secondly, in a solid semiconducting medium the parameter  $\gamma$  becomes

$$\gamma^* = \frac{\ell_{\text{rel}}}{a_B^*} = \frac{m^*}{\epsilon m} \gamma, \quad (25)$$

$\gamma$  being the vacuum value. Thus, using  $\ell_{\text{rel}} \simeq 363.5 (B/\text{Tesla})^{-1/2} \text{ \AA}$  and the values  $\epsilon \simeq 12.4$  and  $m^*/m = 0.067$  for a GaAs heterostructure, we find that the minimum is present in  $V_{\text{eff}}(r)$  for all values of magnetic field *lower* than  $B_{\text{crit}} \simeq 20 \text{ Tesla}$ .

#### IV. THE PAIRED PHASE IN A MAGNETIC FIELD

We return to the circular cell model to develop a variational approach to the total energy in the case of a localized paired phase in a spin-singlet configuration. Two electrons are placed inside each disk of radius  $r_{\text{ws}}$ , the pair wave function being taken in the form

$$\psi_{\kappa,\sigma}(\mathbf{r}_1, \mathbf{r}_2) = \mathcal{A}_{\kappa,\sigma} \left( 1 + \kappa \frac{|\mathbf{r}_1 - \mathbf{r}_2|}{\sigma} \right) \exp \left( -\frac{r_1^2 + r_2^2}{4\sigma^2} \right). \quad (26)$$

where  $\kappa$  and  $\sigma$  are variational parameters and  $\mathcal{A}_{\kappa,\sigma}$  is a normalization constant. The single-pair case treated in Section III is recovered by setting  $\sigma = \ell$  and  $\kappa = 1/\sqrt{2}$ . Notice that the relative motion of the two electrons is described in Eq. (26) by a Gaussian factor times a linear superposition of the Hermite polynomials of zeroth and first order: thus the *Ansatz* (26) allows level mixing due to the electron-electron interactions and is the natural extension of the variational-width method used for the unpaired phase in Section II. More refined wave function would include higher-order Hermite polynomials in the mixing, weighted by additional variational parameter.

The main properties of the wave function (26) are as follows. Firstly, normalization to two electrons per cell yields

$$\mathcal{A}_{\kappa,\sigma} = \left[ \sqrt{2} \pi \sigma^2 (1 + 2\kappa \sqrt{\pi} + 4\kappa^2)^{1/2} \right]^{-1}. \quad (27)$$

Secondly, the most probable value of the relative distance between the two electrons, as obtained from the appropriate maximum of the square of the pair wave function, is

$$|\mathbf{r}_2 - \mathbf{r}_1|_{mp} = \left( \sqrt{1 + 16\kappa^2} - 1 \right) \frac{\sigma}{2\kappa}. \quad (28)$$

This increases with  $\kappa$  and saturates to the value  $2\sigma$ . Thirdly, the single-particle density  $\rho_{\kappa,\sigma}(r) = \int d^2r' |\psi_{\kappa,\sigma}(\mathbf{r}, \mathbf{r}')|^2$  can be obtained in closed form (see Appendix), with the result

$$\rho_{\kappa,\sigma}(r) = \pi \sigma^2 \mathcal{A}_{\kappa,\sigma}^2 e^{-3r^2/4\sigma^2} \left\{ 2 \left( 1 + 2\kappa^2 + \kappa^2 \frac{r^2}{\sigma^2} \right) e^{r^2/4\sigma^2} + \kappa \sqrt{2\pi} \left[ \left( 2 + \frac{r^2}{\sigma^2} \right) I_0\left(\frac{r^2}{4\sigma^2}\right) + \frac{r^2}{\sigma^2} I_1\left(\frac{r^2}{4\sigma^2}\right) \right] \right\}. \quad (29)$$

This expression tends to the correct value  $\rho_{\kappa=0,\sigma}(r) = (\pi \sigma^2)^{-1} \exp(-r^2/2\sigma^2)$  for  $\kappa \rightarrow 0$ .

We proceed to evaluate the total energy per electron associated with the wave function (26). We have

$$\epsilon_t = \frac{1}{2}(\epsilon_{eb} + \epsilon_{bb} + \epsilon_{\text{pair}}), \quad (30)$$

where for the background-background term we can use the result in Eq. (6). The electron-background term is evaluated, as in the calculation performed in Section II.A, from the electrical potential  $V_{\kappa,\sigma}(r)$  created by the electron distribution  $\rho_{\kappa,\sigma}(r)$  in Eq. (29) according to

$$\begin{aligned}
\epsilon_{eb} &= 2\pi n_s \int_0^{r_{\text{WS}}} r dr V_{\kappa,\sigma}(r) \\
&= -\frac{4\alpha}{r_s} \int_0^\infty \frac{dx}{x} \tilde{\rho}_{\kappa,\sigma}(x) J_1(r_{\text{WS}} x/\sigma) Ryd^*
\end{aligned} \tag{31}$$

(see Appendix), where  $J_n(x)$  are Bessel functions. Here

$$\begin{aligned}
\tilde{\rho}_{\kappa,\sigma}(x) &= \frac{1}{2} \sum_{i=1}^2 \langle \psi_{\kappa,\sigma} | e^{-i\mathbf{x}\cdot\mathbf{r}_i/\sigma} | \psi_{\kappa,\sigma} \rangle \\
&= \frac{2 e^{-x^2/2}}{1 + 2\kappa\sqrt{\pi} + 4\kappa^2} \left\{ 1 + 4\kappa^2 - \kappa^2 x^2 - \frac{\sqrt{\pi}}{2} \kappa e^{x^2/8} [(x^2 - 4)I_0(x^2/8) - x^2 I_1(x^2/8)] \right\}.
\end{aligned} \tag{32}$$

In the limit of strong localization ( $\sigma \ll r_{\text{WS}}$ ), we obtain the harmonic-approximation result

$$\epsilon_{eb}^{\text{HA}} = \left[ -\frac{8\alpha}{r_s} + \frac{2\Sigma^2}{\alpha r_s^3} \frac{2 + 5\kappa\sqrt{\pi} + 12\kappa^2}{1 + 2\kappa\sqrt{\pi} + 4\kappa^2} \right] Ryd^*. \tag{33}$$

The same limiting result can be obtained from the electrical potential  $V_{\text{in}}(r)$  created by the background disk, which is still given by Eq. (5).

Finally the contribution  $\epsilon_{\text{pair}}$  in Eq. (30) is given by

$$\begin{aligned}
\epsilon_{\text{pair}} &= \frac{1}{2} \langle \psi_{\kappa,\sigma} | \mathcal{H} | \psi_{\kappa,\sigma} \rangle \\
&= \frac{1}{2} \mathcal{A}_{\kappa,\sigma}^2 \left( \langle \phi_{\text{rel}} | \phi_{\text{rel}} \rangle \langle \phi_{\text{CM}} | \mathcal{H}_{\text{CM}} | \phi_{\text{CM}} \rangle + \langle \phi_{\text{CM}} | \phi_{\text{CM}} \rangle \langle \phi_{\text{rel}} | \mathcal{H}_{\text{rel}} | \phi_{\text{rel}} \rangle \right),
\end{aligned} \tag{34}$$

the center-of-mass and relative motion states and Hamiltonians being immediately obtained from Eqs. (22) and (26). The result is

$$\epsilon_{\text{pair}} = \left( \frac{1}{2\Sigma^2} \frac{2 + 3\kappa\sqrt{\pi} + 8\kappa^2}{1 + 2\kappa\sqrt{\pi} + 4\kappa^2} + 2\lambda_B \Sigma^2 \frac{2 + 5\kappa\sqrt{\pi} + 12\kappa^2}{1 + 2\kappa\sqrt{\pi} + 4\kappa^2} + \frac{\sqrt{\pi}}{\Sigma} \frac{1 + 4\kappa/\sqrt{\pi} + 2\kappa^2}{1 + 2\sqrt{\pi}\kappa + 4\kappa^2} \right) Ryd^*. \tag{35}$$

The last term in this equation arises from the electron-electron interaction.

## V. TOTAL ENERGY OF THE PAIRED PHASE

The total variational energy per electron in the paired circular-cell approximation is obtained from Eqs. (30), (31), (35) and (6). It depends on the three variational parameters  $\Sigma = \sigma/a_B^*$ ,  $\alpha = r_{\text{WS}}/(r_s a_B^*)$  and  $\kappa$ . The equilibrium values of  $\Sigma$  and  $\alpha$  as functions of  $r_s$  show the same trends as displayed in Figure 1 for the unpaired phase. However, the asymptotic value of  $\bar{\Sigma}$  for an electron pair is reduced by a factor of  $\sqrt{2}$  and that of  $\bar{\alpha}$  is  $\bar{\alpha} = \sqrt{\pi}/2$ , increased by a factor  $\sqrt{2}$  over the unpaired state as one expects from the double occupancy of the cell. Internal consistency of the theory is ensured by the ratio  $(\sigma/r_{\text{WS}})_{\text{eq}}$  being smaller than about 0.5, both in the full calculation and in the harmonic approximation, for values of  $r_s > 1$  and of the field  $B > 5$  Tesla. The equilibrium value of  $\kappa$  as a function of  $r_s$  is displayed in Figure 4 for two values of the field. The two electrons in each cell are pushed closer together as the magnetic field increases, leading from Eq. (28) to a decrease of  $\bar{\kappa}$  with increasing field as is shown in Figure 5.

Figure 6 reports the energy  $\delta\epsilon_t$  of the paired phase (that is, after subtraction of the kinetic energy in the lowest LL and reduction to  $e^2/(\epsilon\ell)$  energy units) as a function of the filling factor extending up to  $\nu = 1.5$ . The residual dependence of  $\delta\epsilon_t$  on the magnetic field extends into the high- $r_s$  (low- $\nu$ ) regime, as illustrated in the inset in Figure 5 on a magnified scale, and a finite value is attained by  $\delta\epsilon_t$  as  $\nu \rightarrow 0$ . These features are a consequence of the Coulomb interaction between the two electrons inside each cell. The result in Figure 6 have been fitted to the functional form  $\delta\epsilon_t = f(\nu) e^2/(\epsilon\ell)$ , where

$$f(\nu) = \frac{a\nu^{1/2} + b\nu^{3/2} + c\nu^{5/2} + d}{e\nu^{1/2} + f}. \tag{36}$$

The values of the coefficients in this fitting formula are reported in Table I for various values of the magnetic field.

Figure 7 compares the energies per electron of the unpaired and paired phases as functions of  $r_s$ . The two curves cross at two values of  $r_s$  for each value of the field, but the crossing at lower  $r_s$  is to be discarded as it corresponds to situations where charge leakage out of the circular cell is unacceptably high ( $(\sigma/r_{ws})_{eq} \approx 1$ ). The conclusion from the physically significant crossing at larger  $r_s$ , therefore, is that at each value of the magnetic field in the range from 5 to 20 Tesla the paired phase becomes stable relative to the unpaired one as  $r_s$  decreases.

From the location of the physically acceptable crossing of the energies of the two phases in Figure 7 we obtain their phase boundary in the  $(r_s, \lambda_B)$  plane, which is reported in Figure 8. This shows a region of thermodynamic stability for the paired phase (at least relative to the unpaired one) in the left portion of the plane, before charge leakage outside the cell boundary is expected to occur in an important way so that the model becomes unreliable (to the left of the dash-dotted line in the Figure). Within numerical accuracy we find that the boundary between the two phases is actually set by the  $\nu = 1$  line in the plane<sup>27</sup>. Therefore, the present simple model predicts that electron clusterization may occur only in Landau levels above the lowest one. Of course, the unpaired state in the  $\nu < 1$  region (on the right of the  $\nu = 1$  line) could become stable against the Laughlin liquid only for  $\nu < 0.25$ , as already discussed in connection with Figure 3.

We should emphasize that the ground-state energy difference that we estimate between the paired and the unpaired state is quite appreciable as long as the magnetic field intensity lies in the range that we have illustrated in our calculations. The difference decreases with the field intensity, so that more refined calculations would be needed at low fields.

## VI. SUMMARY AND CONCLUSIONS

We have presented a variational study which approximately accounts for the ground-state energetics of a 2D many-electron system with Coulomb interactions at low density and in the presence of a perpendicular magnetic field. The method consists of an improved 2D version of the well-known spherical cell approximation and is applied to two distinct situations, a single-electron state and a spin-singlet paired state. For the former it gives new analytical and numerical results which are in close agreement with the state-of-the-art calculations on the 2D Wigner crystal.

The evaluation of the spin-paired state has been motivated by previous studies and suggests that this state may be stable in a range of system parameters corresponding to Landau levels above the lowest one. It remains to be seen whether such a paired state would be confirmed in more sophisticated treatments allowing in particular for inter-cell corrections. It may be also emphasized at this point that we have not examined the stability of the spin-singlet paired state against the emergence of spin-polarized states. Evidence from measurements of Knight shift of the  $^{71}\text{Ga}$  nuclei in n-doped GaAs<sup>29</sup> indicates that this quantity, which is proportional to the spin polarization, drops precipitously on either side of  $\nu = 1$ , which is evidence that the charged excitations of the  $\nu = 1$  ground state are finite-size Skyrmions.

## ACKNOWLEDGMENTS

This work was partially supported by MURST through the PRIN Initiative. One of us (M.P.) wishes to thank the Physics Department of the University of Cyprus for their hospitality during part of this work.

## APPENDIX. DETAILS OF ANALYTIC CALCULATIONS

We report in this Appendix some details on the derivation of some analytic results given in the main text.

### A. Equations (10) and (11)

The single-electron potential  $V_{\text{SP}}(r)$  is

$$V_{\text{SP}}(r) = -(2 a_B^* / \sigma) \int_0^{+\infty} dx \tilde{\rho}_{\text{SP}}(x) J_0(x r / \sigma) \quad (37)$$

(in  $Ryd^*$ ), where

$$\tilde{\rho}_{\text{SP}}(x) = \int d^2 r \phi_{\text{SP}}^2(r) J_0(x r / \sigma) = \exp(-x^2/4). \quad (38)$$



Equation (10) in the main text follows by using the result

$$\int_0^{+\infty} \exp(-x^2/4) J_0(ax) dx = \sqrt{\pi} \exp(-a^2/2) I_0(a^2/2). \quad (39)$$

Finally, the integral in Eq. (9) is carried out with the help of the relation

$$\int_0^b x \exp(-x^2/2) I_0(x^2/2) dx = \frac{b^2}{2} e^{-b^2/2} [I_0(b^2/2) + I_1(b^2/2)]. \quad (40)$$

leading to Eq. (11) in the main text.

### B. Equation (29)

The single-particle density  $\rho_{\kappa,\sigma}(r)$  is calculated from the expression

$$\rho_{\kappa,\sigma}(r) = 2\sigma^2 \mathcal{A}_{\kappa,\sigma}^2 \exp(-r^2/\sigma^2) \int_0^{2\pi} d\theta \int_0^{+\infty} x dx (1 + \kappa x)^2 \exp(-x r \cos \theta / \sigma - x^2/2). \quad (41)$$

Eq. (29) is obtained by using the results

$$\int_0^{2\pi} \exp(-xy \cos \theta) d\theta = 2\pi I_0(xy) \quad (42)$$

and

$$\begin{aligned} & \int_0^{+\infty} x (1 + \kappa x)^2 \exp(-x^2/2) I_0(xy) dx = \\ & = \exp(y^2/4) \left\{ (1 + 2\kappa^2 + \kappa^2 y^2) \exp(y^2/4) + \kappa \sqrt{\pi/2} \left[ (2 + y^2) \sqrt{\pi/2} I_0(y^2/4) + y^2 I_1(y^2/4) \right] \right\}. \end{aligned} \quad (43)$$

### C. Equation (31)

The electrical potential  $V_{\kappa,\sigma}(r)$  created by the electron distribution  $\rho_{\kappa,\sigma}(r)$  in Eq. (29) is written as

$$V_{\kappa,\sigma}(r) = -(2a_B^*/\sigma) \int_0^{+\infty} dx \tilde{\rho}_{\kappa,\sigma}(x) J_0(xr/\sigma) \quad (44)$$

(in  $Ryd^*$ ), where in essence  $\tilde{\rho}_{\kappa,\sigma}(x)$  is the Fourier transform of the electron density distribution (see Eq. (32)). After inserting this formula into the first line of Eq. (31) and interchanging the order of the two integrations, the integration over  $r$  can be carried out with the help of the result

$$\int_0^b J_0(ax) x dx = \frac{b}{a} J_1(ab). \quad (45)$$

This yields the second line of Eq. (31) in the main text.

<sup>1</sup> See *e.g.* *The Quantum Hall Effect*, eds. R. E. Prange and S. M. Girvin (Springer, New York 1987); *Perspectives in Quantum Hall Effects*, eds. S. Das Sarma and A. Pinczuk (Wiley, New York 1997).

<sup>2</sup> M. Shayegan, in *Perspectives in Quantum Hall Effects*, eds. S. Das Sarma and A. Pinczuk (Wiley, New York 1997), p. 343.

- <sup>3</sup> M. P. Lilly, K. B. Cooper, J. P. Eisenstein, L. N. Pfeiffer, and K. W. West, Phys. Rev. Lett. **82**, 394 (1999); R. R. Du, D. C. Tsui, H. L. Stormer, L. N. Pfeiffer, K. W. Baldwin, and K. W. West, Solid State Commun. **109**, 389 (1999); K. B. Cooper, M. P. Lilly, J. P. Eisenstein, L. N. Pfeiffer, and K. W. West, Phys. Rev. B **60**, R11285 (1999).
- <sup>4</sup> A. A. Koulakov, M. M. Fogler, and B. I. Shklovskii, Phys. Rev. Lett. **76**, 499 (1996); M. M. Fogler, A. A. Koulakov and B. I. Shklovskii, Phys. Rev. B **54**, 1853 (1996); R. Moessner and J. T. Chalker, Phys. Rev. B **54**, 5006 (1996); M. M. Fogler and A. A. Koulakov, Phys. Rev. B **55**, 9326 (1997).
- <sup>5</sup> F. D. M. Haldane, E. H. Rezayi, and Kun Yang, Phys. Rev. Lett. **85**, 5396 (2000).
- <sup>6</sup> N. Shibata and D. Yoshioka, Phys. Rev. Lett. **86**, 5755 (2001).
- <sup>7</sup> S. M. Girvin, *The Quantum Hall Effect: Novel Excitations and Broken Symmetries*, Lectures at Ecole d'Eté Les Houches (1998).
- <sup>8</sup> M. Taut, Phys. Rev. A **48**, 3561 (1993); M. Taut, J. Phys. A **27**, 1045 and 4723 (1994); M. Taut, J. Phys.: Condens. Matter **12**, 3689 (2000).
- <sup>9</sup> G. V. Shuster and A. I. Kozinskaya, Fiz. Tverd. Tela **13**, 1240 (1971) [Sov. Phys. Solid State **13**, 1038 (1971)].
- <sup>10</sup> K. Mouloupoulos and N. W. Ashcroft, Phys. Rev. B **48**, 11646 (1993).
- <sup>11</sup> G. M. Summers, R. J. Warburton, J. G. Michels, R. J. Nicholas, J. J. Harris, and C. T. Foxon, Phys. Rev. Lett. **70**, 2150 (1993); R. B. Dunford, E. E. Mitchell, R. G. Clark, V. A. Stadnik, F. F. Fang, R. Newbury, R. H. McKenzie, R. P. Starrett, P. J. Wang, and B. S. Meyerson, J. Phys.: Condens. Matter **9**, 1565 (1997).
- <sup>12</sup> See, *e.g.* Appendix A in Ref. 10 for the 3D version of the cell approximation in zero magnetic field. A spherical cell is there exploited in both a point-charge and a distributed-charge approach, to deal with the WC and with an orientationally symmetric paired crystalline phase.
- <sup>13</sup> I. Nagy, Phys. Rev. B **60**, 4404 (1999).
- <sup>14</sup> Y. E. Lozovik and V. I. Yudson, JEPT Lett. **22**, 11 (1975).
- <sup>15</sup> L. Bonsall and A. A. Maradudin, Phys. Rev. B **15**, 1959 (1977); E. Cockayne and V. Elser, Phys. Rev. B **43**, 623 (1991).
- <sup>16</sup> D. Yoshioka and H. Fukuyama, J. Phys. Soc. Jpn. **47**, 394 (1979); D. Yoshioka and P. A. Lee, Phys. Rev. B **27**, 4986 (1983); K. Maki and X. Zotos, Phys. Rev. B **28**, 4349 (1983).
- <sup>17</sup> D. Levesque, J. J. Weis, and A. H. MacDonald, Phys. Rev. B **30**, 1056 (1984).
- <sup>18</sup> P. K. Lam and S. M. Girvin, Phys. Rev. B **30**, 473 (1984).
- <sup>19</sup> G. Vignale, Phys. Rev. B **47**, 10105 (1993).
- <sup>20</sup> *Handbook of Mathematical Functions*, eds. M. Abramowitz and I. A. Stegun (Dover, New York 1972).
- <sup>21</sup> D. C. Tsui, H. L. Stormer and A. C. Gossard, Phys. Rev. Lett. **48**, 1559 (1982); E. Y. Andrei, G. Deville, D. C. Glattli, F. I. B. Williams, E. Paris and N. Etienne, Phys. Rev. Lett. **60**, 2765 (1988); R. L. Willett, H. L. Stormer, D. C. Tsui, L. N. Pfeiffer, K. W. West and K. W. Baldwin, Phys. Rev. B **38**, 7881 (1988); H. W. Jiang, R. L. Willett, H. L. Stormer, D. C. Tsui, L. N. Pfeiffer and K. W. West, Phys. Rev. Lett. **65**, 633 (1990); H. W. Jiang, H. L. Stormer, D. C. Tsui, L. N. Pfeiffer and K. W. West, Phys. Rev. B **44**, 8107 (1991); V. J. Goldman, M. Santos, M. Shayegan and J. E. Cunningham, Phys. Rev. Lett. **65**, 2189 (1990); D. C. Glattli, G. Deville, V. Duburcq, F. I. B. Williams, E. Paris, N. Etienne and E. Y. Andrei, Surf. Sci. **229**, 344 (1990); H. Buhmann, W. Joss, K. von Klitzing, I. V. Kukushkin, A. S. Plaut, G. Martinez, K. Ploog and V. Timofeev, Phys. Rev. Lett. **66**, 926 (1991); F. I. B. Williams, P. A. Wright, R. G. Clark, E. Y. Andrei, G. Deville, D. C. Glattli, O. Probst, B. Etienne, C. Dorin, C. T. Foxon and J. J. Harris, Phys. Rev. Lett. **66**, 3285 (1991); R. L. Willett, M. A. Paalanen, R. R. Ruel, K. W. West, L. N. Pfeiffer and D. J. Bishop, Phys. Rev. Lett. **65**, 112 (1990).
- <sup>22</sup> X. Zhu and S. G. Louie, Phys. Rev. Lett. **70**, 335 (1993).
- <sup>23</sup> R. Price, X. Zhu, S. Das Sarma, and P. M. Platzman, Phys. Rev. B **51**, 2017 (1995).
- <sup>24</sup> M. Seidl, J. P. Perdew, and M. Levy, Phys. Rev. A **59**, 51 (1999); M. Seidl and J. P. Perdew, Phys. Rev. B **50**, 5744 (1994).
- <sup>25</sup> E. H. Lieb and H. Narnhofer, J. Stat. Phys. **12**, 291 (1975).
- <sup>26</sup> A. Turbinger, Phys. Rev. A **50**, 5335 (1994).
- <sup>27</sup> The lines of constant  $\nu$  in the  $(r_s, \lambda_B)$  plane are described by the equation  $\lambda_B = 1/(\nu^2 r_s^4)$ , so that the line  $\nu = 1$  in Figure 8 separate the lowest LL (on its right) from the higher ones (on its left).
- <sup>28</sup> S. L. Sondhi, A. Karlhede, S. A. Kivelson and E. H. Rezayi, Phys. Rev. B **47**, 16419 (1993).
- <sup>29</sup> S. E. Barrett, G. Dabbagh, L. N. Pfeiffer, K. W. West, and R. Tycko, Phys. Rev. Lett. **74**, 5112 (1995).

TABLE I. Coefficients of the interpolation formula in Eq. (36).

B (Tesla)	$a$	$b$	$c$	$d$	$e$	$f$
5	-0.6621	0.2769	-0.0647	0.1751	-0.0072	0.5578
10	-0.6435	0.2715	-0.0588	0.1828	-0.0231	0.5406
15	-0.6325	0.2655	-0.0548	0.1869	-0.0288	0.5302
20	-0.6255	0.2612	-0.0522	0.1894	-0.0315	0.5237

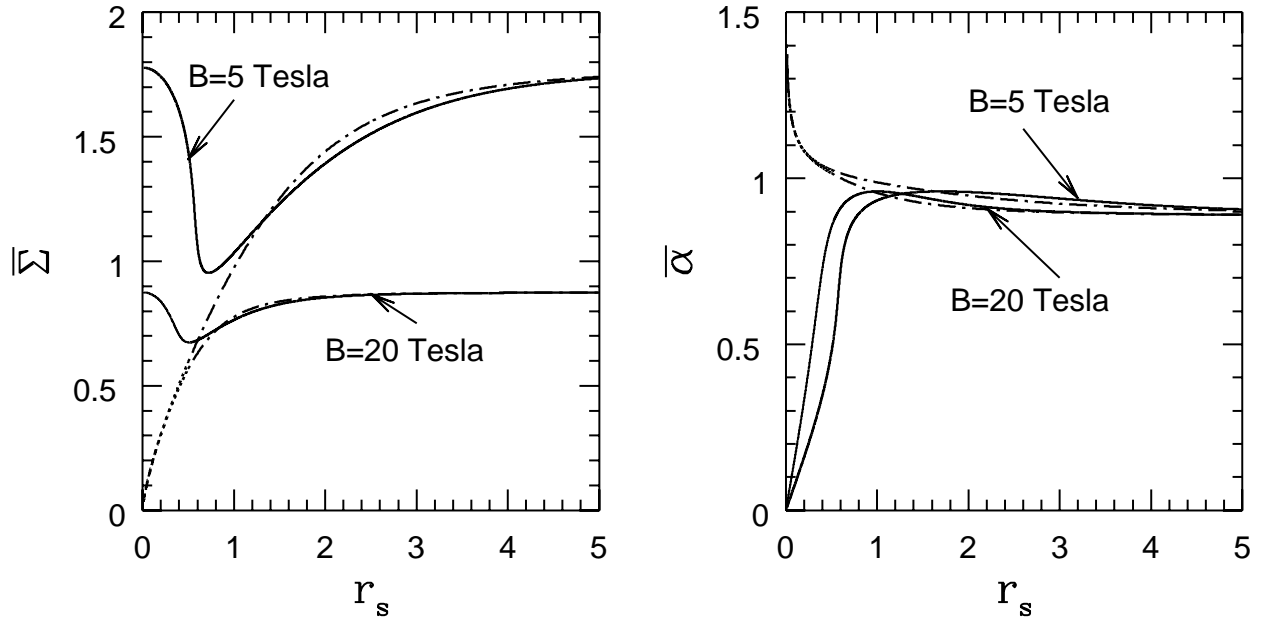


FIG. 1. Equilibrium values of the reduced width  $\bar{\Sigma} \equiv (\sigma/a_B^*)_{\text{eq}}$  (left panel) and of the reduced disk radius  $\bar{\alpha} \equiv (r_{\text{WS}}/r_s a_B^*)_{\text{eq}}$  (right panel) as functions of  $r_s$  and for two values of the magnetic field. The asymptotic values at large  $r_s$  are  $\sigma_{\text{eq}} = (\hbar/m^* \omega_0)^{1/2}$  and  $\bar{\alpha} = \sqrt{\pi}/2$ , the latter being the value obtained by Nagy<sup>13</sup> in zero field. The dot-dashed lines are obtained from the harmonic approximation, which is becoming approximately valid for  $r_s \geq 1$ .

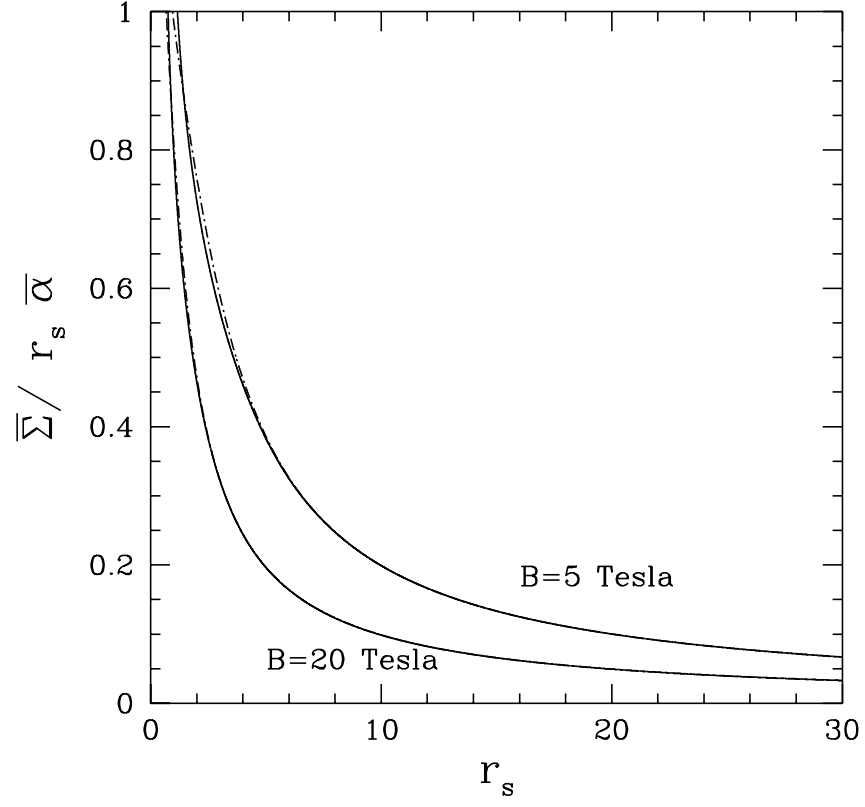


FIG. 2. Consistency ratio  $\bar{\Sigma}/(r_s \bar{\alpha})$  as a function of  $r_s$  for two values of the magnetic field. The dot-dashed lines are obtained from the harmonic approximation.

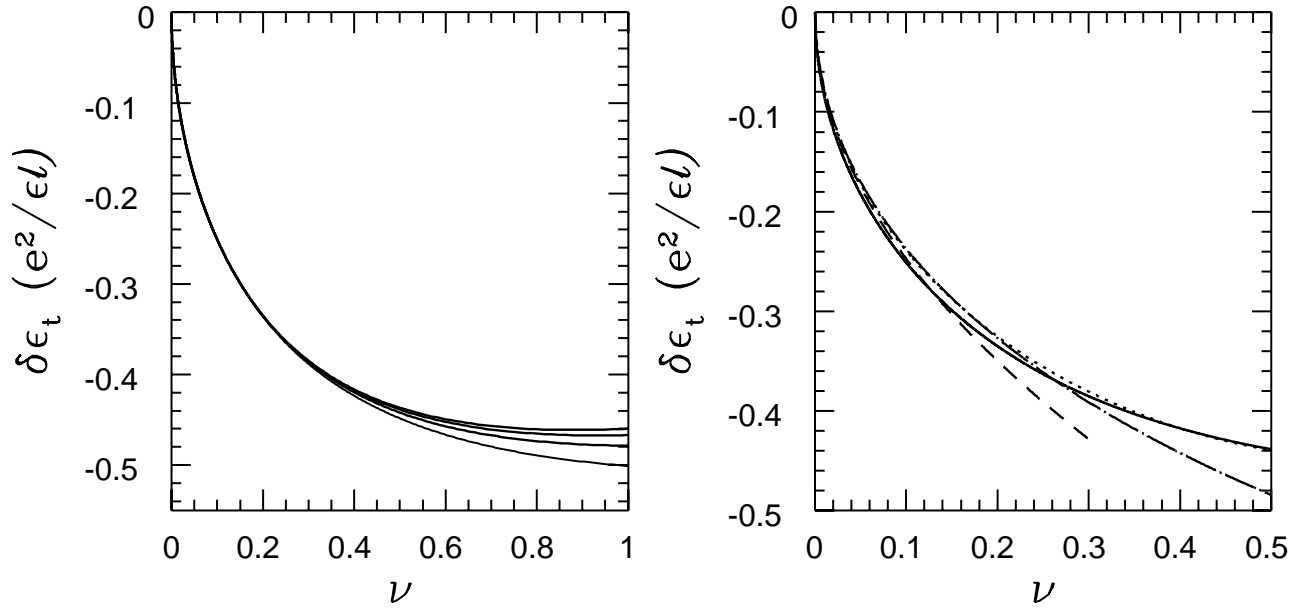


FIG. 3. Left panel: Ground-state energy  $\delta\epsilon_t$  of the unpaired WC, in units of  $e^2/\epsilon\ell$ , as a function of the filling factor  $\nu$  in the range  $0 < \nu \leq 1$  for values of  $B = 5, 10, 15$  and  $20$  Tesla (from bottom to top). Right panel: Ground-state energy of the unpaired WC obtained in the present approach (full line) compared with the CWC result of Lam and Girvin (dotted line), with the asymptotic classical result (dashed line) and with the energy of the Laughlin liquid (dot-dashed line, from Levesque *et al.*).

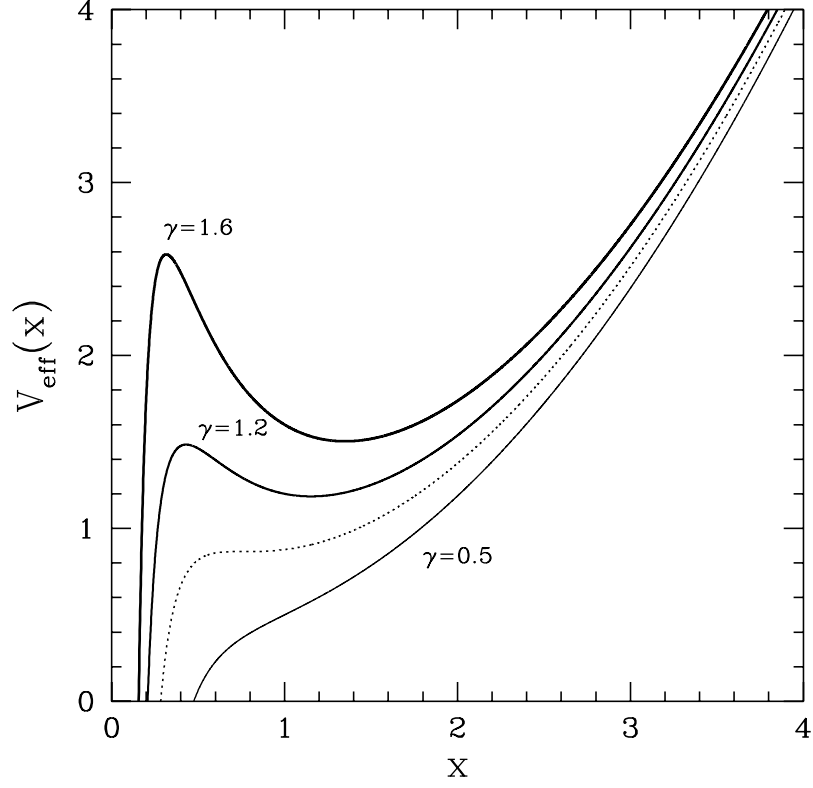


FIG. 4. Effective potential  $V_{\text{eff}}(r)$  for the relative motion at zero relative angular momentum. The dotted line corresponds to the critical value  $\gamma_{\text{crit}} = (16/27)^{1/4}$ , above which a minimum is present. The dotted line has an inflection point at  $x_{\text{crit}} = 2/(3\gamma_{\text{crit}})$ .

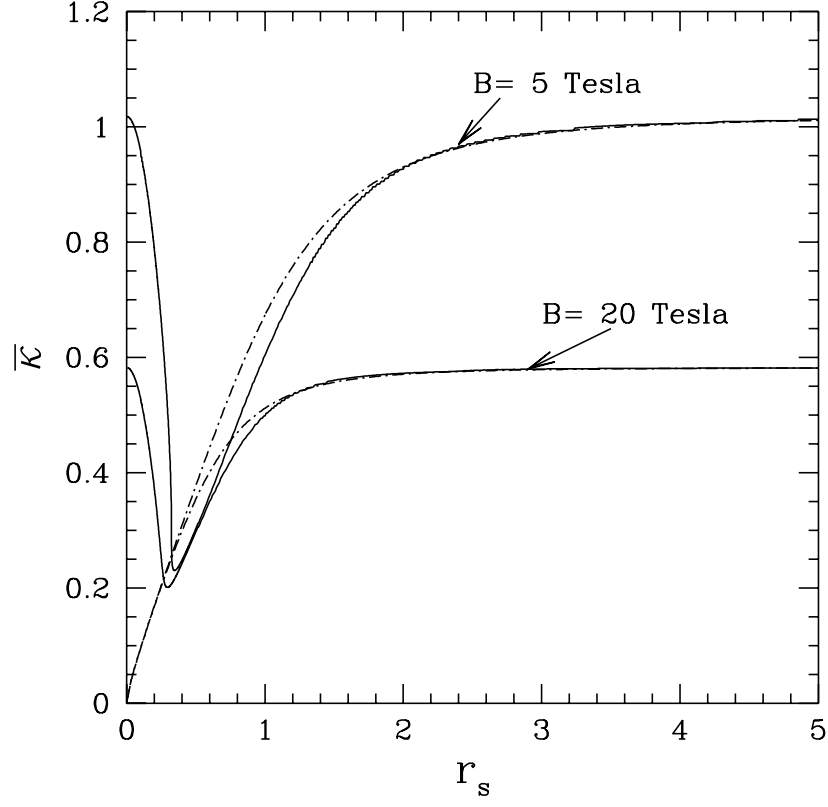


FIG. 5. The parameter  $\bar{\kappa}$  as a function of  $r_s$  for two values of the field  $B$  in the paired phase (full lines). The dash-dotted lines show the results of the harmonic approximation.



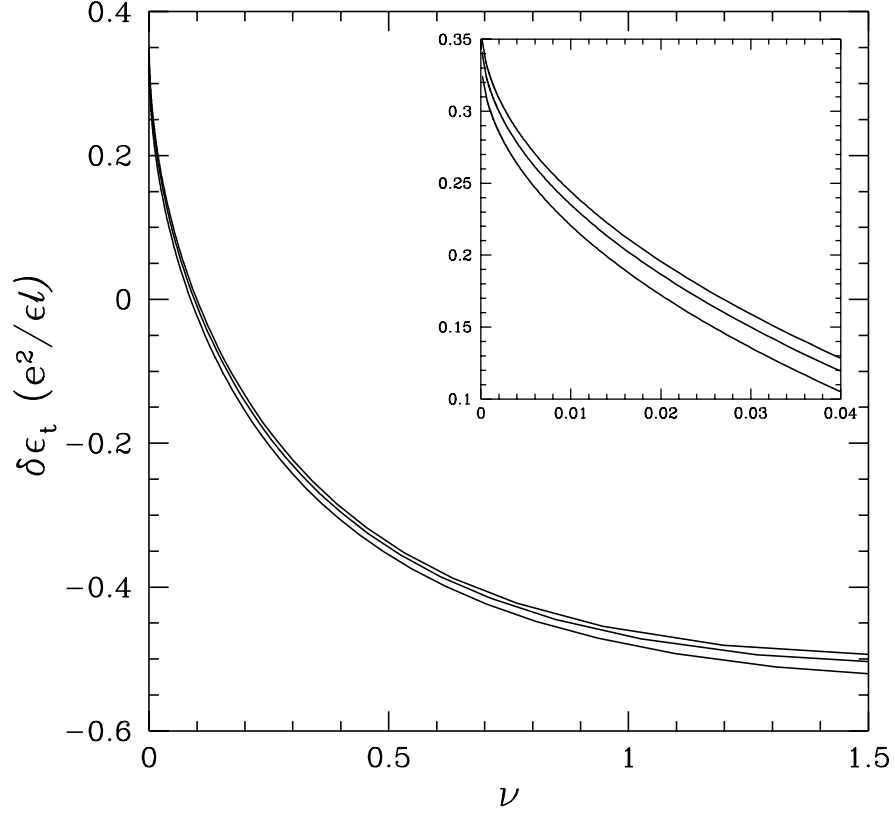


FIG. 6. The energy  $\delta\epsilon_t$  of the paired phase as a function of the filling factor  $\nu$  for various values of the magnetic field (increasing from 10 to 20 Tesla from bottom to top). The inset shows an enlarged view of the region  $\nu \rightarrow 0$ .

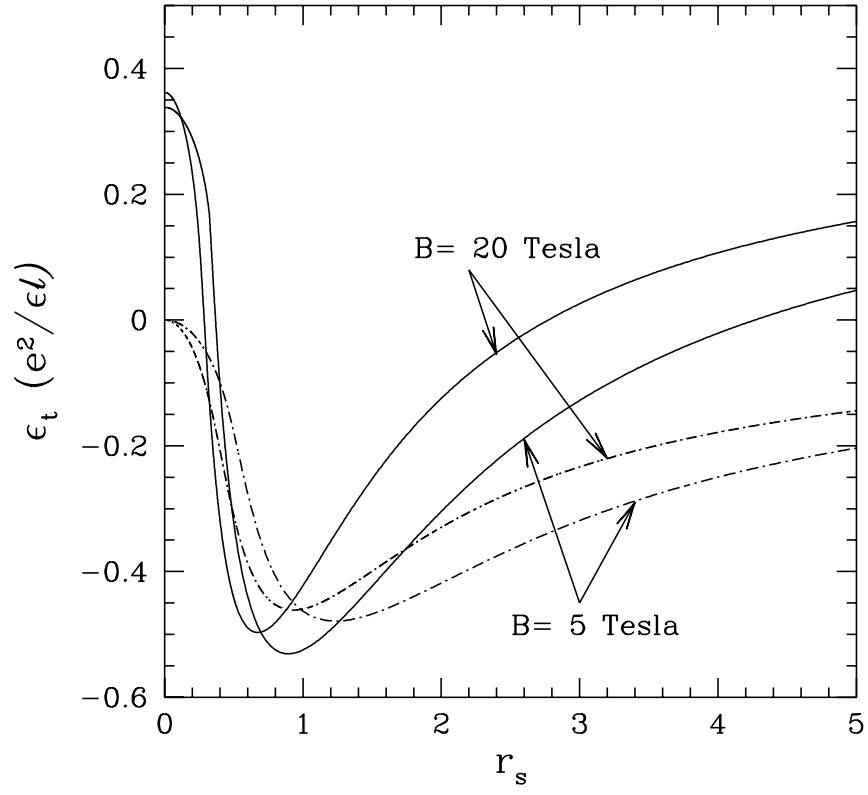


FIG. 7. Comparison of the total energies of the paired state (full lines) and of the unpaired state (dash-dotted lines) for two values of the magnetic field.

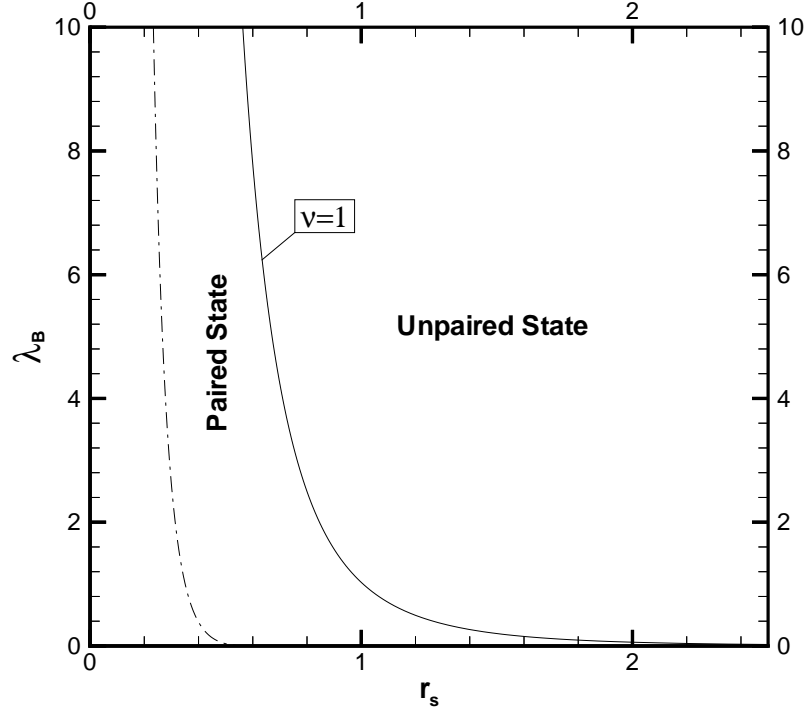


FIG. 8. Boundary between the singlet-spin paired state and the unpaired state in the  $(r_s, \lambda_B)$  plane. The boundary is set by the  $\nu = 1$  line. The dash-dotted line shows where the consistency ratio  $\bar{\Sigma}/r_s\bar{\alpha}$  for the paired state becomes unity.